

Simple cluster mean-field theory for disordered systems: Off-diagonal disorder in substitutional alloys

Rafael E. Peña

Seiscom Delta United Inc., Corporate Research, P.O. Box 4610, Houston, Texas 77210

(Received 28 April 1983; revised manuscript received 4 November 1983)

We have developed a cluster-effective-medium approach for the numerical computation of the physical properties of systems with diagonal and off-diagonal disorder including short-range order. Our embedding technique, which is equivalent to one first discovered by Kumar and Joshi, treats the cluster systematically within a hierarchical scheme for the propagators. Dependent on cluster size, the highest-order propagator in the hierarchy is approximated by that belonging to the statistically averaged effective medium. Expressions for observables are obtained as functions of effective-medium quantities. The effective medium is then chosen to satisfy the exact dispersion relations and the first few sum rules which analyticity in the complex-frequency plane requires of the exact, translationally invariant quasiparticle self-energy $\Sigma(\vec{k}, \omega)$. The sum rules are fixed by the \vec{k} -diagonal matrix elements, $(H^n)_{\vec{k}, \vec{k}}$ of the Hamiltonian. These matrix elements are self-averaged and therefore may be computed directly from knowledge of the distribution functions characterizing the translationally invariant disorder. Numerical results for off-diagonal disorder in a one-dimensional binary alloy within the single-site-cluster approximation are included. The theory is self-consistent in an iterative sense and is analytic by construction so that propagators are necessarily free of any pathologic singularities. Beyond its present application to off-diagonal disorder in substitutional systems, the theory also encompasses short-range order in amorphous systems.

I. INTRODUCTION

A general comprehensive theory for the behavior of excitations in disordered media will be expected to meet a long list of requirements. To name a few, the theory must be causal, so that stringent analyticity conditions must be satisfied by all averaged propagators. If the distribution of disorder is translationally invariant, so too must be the predicted macroscopic physical observables; constraints emerge on the definition of the effective medium and the technique by which the cluster is embedded within it. The exact limiting behaviors at weak or strong scattering and high or low concentrations must be reproduced. The formalism should place no *ab initio* restrictions on the number of distinct microscopic components comprising the system nor should it restrict the short-range character of the disorder distribution functions. One-particle and two-particle properties should be computable within essentially the same framework. If desired, the theory should be implementable in a self-consistent mode. Finally, it should incorporate sufficient parameter flexibility to accommodate, for instance, the self-consistent many-body screening of the electronic problem.

To date, despite many important advances, the search for such a comprehensive theory has been unsuccessful. Many difficulties have been encountered;¹ the principal one has been a proper definition of the effective medium and its relation to the cluster embedded within. The discovery of the coherent-potential approximation (CPA), for single-site scattering, by Soven and Taylor,^{2,3} was followed by attempts to specify effective mediums such that arbitrarily large embedded clusters would, in some sense,

fail to scatter. Those works were inspired in part by the impressive success of CPA and because the average T matrix must vanish in an exact theory.⁴ The earlier efforts pursued a rather straightforward implementation of the non-scattering-medium idea in the construction of multiple-scattering generalizations to the CPA.¹ That period was brought to an end by the work of Nickel and Butler,⁵ who clearly demonstrated the implausibility of satisfying both *ab initio* self-consistency and causality via direct approximate methods.

Two schools of thought have emerged in response to this state of affairs. The first, influenced by Mills and Ratanavararaksa,⁶ relies on diagrammatic techniques to obtain approximations which are both *ab initio* self-consistent and analytic. In conjunction with the augmented-space techniques of Mookerjee,^{7,8} important progress has been made.⁹⁻¹² These works, however, are not yet generally practicable. Their authors have experienced considerable difficulty with the treatment of correlated disordered systems, offering at present only a perturbative solution.¹² From a computational point of view, what is perhaps of most concern are the theoretical complexities to which a worker must subject himself to obtain numbers. It would appear that the theory will be significantly more involved in applications to amorphous and geophysical systems of current interest.

The second school of thought, to which this work belongs, sacrifices *ab initio* self-consistency in favor of guaranteed analyticity.¹³⁻¹⁸ The cluster propagators are computed in terms of yet undetermined medium propagators. The result is a theory which is flexible and general. It will accommodate diagonal and off-diagonal disorder as

well as environmental disorder. Short-range order is also simply incorporated and the generalization to amorphous disorder is relatively straightforward. Furthermore, numerical implementation is simple. However, one glaring problem remains: What should be used for an effective medium? Some suggestions have been a Bethe lattice,¹³⁻¹⁵ the effective medium from the single-site CPA,¹⁶ or simple functional forms motivated by the CPA results.^{17,18}

In this paper, we propose a resolution of this effective-medium question, which is based on exact theorems for the quasiparticle self-energy of any particular disorder problem. We use any number (in principle) of the infinite moment equations, which analyticity requires of the exact self-energy $\Sigma(\vec{k}, \omega)$, to fix parameters in simple guessed functional forms for the effective-medium self-energy $\mathcal{E}_1(\vec{k}, \omega)$. An iterative process is thus initiated, where $\mathcal{E}_{n+1}(\vec{k}, \omega)$ is determined from the cluster Green's functions for a given $\mathcal{E}_n(\vec{k}, \omega)$. In this manner self-consistency may be established. However, as shown here and as demonstrated previously,¹³⁻¹⁸ very good results may be obtained after only the first step. The outline of this paper is as follows.

In Sec. II we specify the model which concerns us in this work. The model is a tight-binding Hamiltonian with nearest-neighbor kinetic energy matrix elements. Diagonal and off-diagonal disorder are included together with short-range order in the form of a conditional probability for nearest-neighbor occupancy with a simple Cowley parametrization.¹⁷ Section III presents a detailed discussion of the analytic properties, dispersion relations, and sum rules which causality imposes on the exact quasiparticle self-energy. We use the fact that the \vec{k} -diagonal matrix elements of any power of Hamiltonian are configurationally self-averaged when the distribution of disorder is translationally invariant. Hence, we are able to explicitly evaluate one side of the sum-rule equalities. We note that this sum-rule analysis has appeared previously.¹⁹ In Sec. IV we discuss our technique for embedding the cluster in the effective medium which is yet unspecified. Although formally different, our embedding method is entirely equivalent (Appendix A) to the one which was first discovered by Kumar and Joshi.²⁰ Identification of the cluster Hamiltonian leads to a Lippmann-Schwinger hierarchy of propagator equations. These equations are solved approximately by truncating the hierarchy at any arbitrary point and replacing the highest-order propagator with that belonging to the effective medium. As our numerical results of Sec. VI are for the local density of states in the one-site cluster approximation (ISCA), detailed equations are shown only for truncation at the first level in the propagator hierarchy. Section V concerns our choice of medium. We show that the sum rules completely determine the \vec{k} dependence of the medium self-energy $\mathcal{E}_1(\vec{k}, \omega)$ when a simple and intuitive ansatz is made for its frequency dependence. Our selections for the latter follow those of Bloom and Mattis.^{17,18} Appendix B contains a discussion of conditions which causality imposes on the choice of effective medium. In Sec. VI we illustrate and discuss the information content present in the sum rules

and show first iteration results for the local density of states pertinent to the one-dimensional alloy model of Sec. II. Our ISCA results for diagonal off-diagonal disorder in the strong-scattering, split-band limit compare favorably with corresponding results of Kaplan, Leath, Gray, and Diehl.¹¹ We summarize our findings in Sec. VII.

II. THE MODEL

We consider tight-binding electrons in a binary, substitutionally disordered solid with Hamiltonian

$$\hat{H} = \hat{T} + \hat{V}, \quad \hat{T} = \sum_{i,j=1}^N T_{ij} |i\rangle\langle j|, \quad \hat{V} = \sum_{i=1}^N V_i |i\rangle\langle i|. \quad (2.1)$$

Except where otherwise indicated, our analysis will be applicable to any number of dimensions. The off-diagonal matrix elements T_{ij} take on values of T_{AA} , T_{AB} , T_{BA} , and T_{BB} for nearest-neighbor atoms of both type A or A next to B , or both type B . Similarly, the diagonal V_i assumes the values V_A or V_B . In this work, we take $T_{BA} = T_{AB} \in \mathcal{R}$. We assume that atoms A are found in concentration c_A , and therefore atoms B are found in concentration $c_B = 1 - c_A$. We treat short-range order with a simple Cowley parametrization of the conditional probability for nearest-neighbor occupancy.¹⁷ We note, however, that the theory developed in this work places no *a priori* restrictions on the types of distribution functions which may be used to characterize the short-range order. Cowley's parametrization is

$$\begin{aligned} P(A;A) &= c_A + sc_B, & P(B;A) &= c_B(1-s), \\ P(A;B) &= c_A(1-s), & P(B;B) &= c_B + sc_A. \end{aligned} \quad (2.2)$$

$P(\beta; \alpha)$ is the probability of finding an atom of type β at a nearest-neighbor site of one known to be type α . The allowed range of $s \leq 1$ depends on concentration, and is as such to ensure the semidefinite positivity of the conditional probabilities (2.2). Equations (2.2) satisfy the required

$$\begin{aligned} \sum_{\beta=A,B} P(\beta; \alpha) &= 1, \quad \alpha = A, B \\ \sum_{\alpha=A,B} P(\beta; \alpha) c_\alpha &= c_\beta, \quad \beta = A, B. \end{aligned} \quad (2.3)$$

The numerical results of Sec. VI are for the single-particle density of states of a one-dimensional substitutionally disordered alloy of lattice constant a with Hamiltonian (2.1).

III. EXACT SUM RULES AND DISPERSION RELATIONS

The Schrödinger-equation response function

$$\hat{G}(t) = \begin{cases} e^{-i\hat{H}t}, & t \geq 0 \\ 0, & t < 0 \end{cases} \quad (3.1)$$

has a contour-integral representation in the complex-frequency plane,

$$\hat{G}(t) = \frac{-1}{2\pi i} \oint_C dz e^{-izt} \hat{G}(z), \quad (3.2)$$

$$\hat{G}(z) = \frac{1}{z - \hat{H} + i0^+}. \quad (3.3)$$

The contour C includes the entire real axis, $(-\infty, \infty)$, and closes in the upper half-plane (UHP) for $t < 0$ or the lower half-plane for $t \geq 0$.

The propagator (3.3) is analytic in the UHP, and therefore, so is the matrix element

$$G_{\vec{k}, \vec{k}}(z) = \langle \vec{k} | \hat{G}(z) | \vec{k} \rangle, \quad (3.4)$$

$$| \vec{k} \rangle = \frac{1}{\sqrt{N}} \sum_i e^{i\vec{k} \cdot \vec{r}_i} | i \rangle. \quad (3.5)$$

Formally, we may write Eq. (3.4) as

$$G_{\vec{k}, \vec{k}}(z) = \frac{1}{z} + \frac{1}{z^2} \langle \vec{k} | \hat{H} | \vec{k} \rangle + \frac{1}{z^3} \langle \vec{k} | \hat{H}^2 | \vec{k} \rangle + \dots, \quad (3.6)$$

and note that all the matrix elements on the right-hand side are configurationally self-averaged, i.e.,

$$\langle \vec{k} | \hat{H}^n | \vec{k} \rangle = [\langle \vec{k} | \hat{H}^n | \vec{k} \rangle]_{\text{av}}, \quad n = 1, 2, \dots \quad (3.7)$$

where $[\]_{\text{av}}$ indicates the operation of configurational averaging. A little study reveals (3.7) is due to the fact that \hat{H}^n may always be cast in the form $\sum_{i,j} \hat{O}(\vec{r}_i - \vec{r}_j)$, so that each local configuration contributes to the total sum irrespective of its absolute position in the lattice. For the model of Sec. II, our results for the first three moments in a one-dimensional lattice are

$$\langle k_x | \hat{H} | k_x \rangle = \sum_{\alpha=A,B} c_\alpha \left[V_\alpha + \left[2 \sum_{\beta=A,B} P(\beta; \alpha) T_{\alpha\beta} \right] \cos(ak_x) \right], \quad (3.8)$$

$$\begin{aligned} \langle k_x | \hat{H}^2 | k_x \rangle = & \sum_\alpha c_\alpha \left[\left[V_\alpha^2 + 2 \sum_\beta P(\beta; \alpha) T_{\alpha\beta} T_{\beta\alpha} \right] + \left[2 \sum_\beta P(\beta; \alpha) T_{\alpha\beta} (V_\alpha + V_\beta) \right] \cos(ak_x) \right. \\ & \left. + \left[2 \sum_\beta P(\beta; \alpha) T_{\alpha\beta} \sum_\gamma P(\gamma; \beta) T_{\beta\gamma} \right] \cos(2ak_x) \right], \quad (3.9) \end{aligned}$$

$$\begin{aligned} \langle k_x | \hat{H}^3 | k_x \rangle = & \sum_\alpha c_\alpha \left[\left[V_\alpha^3 + 2 \sum_\beta P(\beta; \alpha) T_{\alpha\beta} T_{\beta\alpha} (2V_\alpha + V_\beta) \right] \right. \\ & \left. + \left[2 \sum_\beta P(\beta; \alpha) T_{\alpha\beta} \left[V_\alpha^2 + V_\alpha V_\beta + V_\beta^2 \right. \right. \right. \\ & \left. \left. + T_{\beta\alpha} \left[T_{\alpha\beta} + \sum_\gamma P(\gamma; \alpha) T_{\alpha\gamma} \right] + \sum_\gamma P(\gamma; \beta) T_{\beta\gamma} T_{\gamma\beta} \right] \right] \cos(ak_x) \\ & + \left[2 \sum_\beta P(\beta; \alpha) T_{\alpha\beta} \sum_\gamma P(\gamma; \beta) T_{\beta\gamma} (V_\alpha + V_\beta + V_\gamma) \right] \cos(2ak_x) \\ & \left. + \left[2 \sum_\beta P(\beta; \alpha) T_{\alpha\beta} \sum_\gamma P(\gamma; \beta) T_{\beta\gamma} \sum_\delta P(\delta; \gamma) T_{\gamma\delta} \right] \cos(3ak_x) \right]. \quad (3.10) \end{aligned}$$

Calculation of these moments is increasingly difficult with higher order and or higher dimension. Evidently, this problem may be overcome by the development of computer algorithms which directly evaluate the various terms enclosed by large parentheses in the above equations. Nevertheless, it is our belief that most applications will require calculation of only the first few moments. As will be seen later in Sec. V, the usefulness of the sum rules is in some measure due to the fact that for a substitutionally disordered system $\langle \vec{k} | \hat{H}^n | \vec{k} \rangle$ may always be cast in the form of a sum of terms, each of which is the product of a probabilistic weight times a topological structure factor. For substitutional disorder, these topological terms are completely independent of the disorder. It is not difficult to see that there exists a class of amorphously disordered systems for which $\langle \vec{k} | \hat{H}^n | \vec{k} \rangle$ also has this con-

venient form. For example, such will be the case for an amorphous system in which each atom has the exact same number of nearest neighbors and in which the substitutional disorder is statistically independent of the topological disorder.

Returning to Eqs. (3.6) and (3.7) we see that

$$[\langle \vec{k} | \hat{G}(z) | \vec{k} \rangle]_{\text{av}} = \frac{1}{z - \Sigma(\vec{k}, z)} = \langle \vec{k} | \hat{G}(z) | \vec{k} \rangle, \quad (3.11)$$

where $\Sigma(\vec{k}, z)$ is the exact quasiparticle self-energy. The configurationally averaged Green's function is therefore analytic in the UHP when the distribution of disorder is translationally invariant, since in that case

$$[\langle \vec{k} | \hat{G}(z) | \vec{k}' \rangle]_{\text{av}} = 0, \quad \vec{k} \neq \vec{k}'. \quad (3.12)$$

It is not difficult to convince oneself that the analyticity of $[G_{\vec{k}, \vec{k}}(z)]_{av}$ in the UHP requires the analyticity of $\Sigma(\vec{k}, z)$ there also. A simple proof of this has been published by Mookerjee.^{8,21} Therefore Cauchy's integral formula

$$\Sigma(\vec{k}, z) = \frac{1}{2\pi i} \oint_C dz' \frac{\Sigma(\vec{k}, z')}{z' - z} \quad (3.13)$$

must be satisfied. In (3.13) and hereafter, the contour C will be taken to enclose the entire UHP.

From (3.6) and (3.11) it may be shown that $\Sigma(\vec{k}, z)$ has a large z expansion of the form

$$\Sigma(\vec{k}, z) = \sum_{n=0}^{\infty} Q_n(\vec{k}) z^{-n}, \quad (3.14)$$

where the coefficients Q_n may be evaluated by equating powers of z in the expression

$$\sum_{n=0}^{\infty} \frac{[\Sigma(\vec{k}, z)]^n}{z^n} = \left\langle \vec{k} \left| \sum_{n=0}^{\infty} \frac{\hat{H}^n}{z^n} \right| \vec{k} \right\rangle. \quad (3.15)$$

Explicitly, the first three terms yield

$$\begin{aligned} Q_0(\vec{k}) &= \langle \vec{k} | \hat{H} | \vec{k} \rangle, \\ Q_1(\vec{k}) &= \langle \vec{k} | \hat{H}^2 | \vec{k} \rangle - [Q_0(\vec{k})]^2, \\ Q_2(\vec{k}) &= \langle \vec{k} | \hat{H}^3 | \vec{k} \rangle - [Q_0(\vec{k})]^3 - 2Q_0(\vec{k})Q_1(\vec{k}), \end{aligned} \quad (3.16)$$

etc. The analyticity of $\Sigma(\vec{k}, z)$ in the UHP and Eq. (3.14) imply that the infinite set of functions

$$\begin{aligned} Y_0(\vec{k}, z) &= \Sigma(\vec{k}, z) - Q_0(\vec{k}), \\ Y_n(\vec{k}, z) &= zY_{n-1}(\vec{k}, z) - Q_n(\vec{k}), \quad n=1, 2, \dots \end{aligned} \quad (3.17)$$

are analytic in the UHP and vanish as $1/z$ when $|z| \rightarrow \infty$. From Cauchy's integral theorem,

$$\oint_C dz Y_n(\vec{k}, z) = 0, \quad n=0, 1, 2, \dots \quad (3.18)$$

we obtain an infinite set of sum rules, the imaginary parts

$$\begin{aligned} \hat{H} &= \hat{H}^{(I)}(z) + \delta \hat{H}^{(I)}(z), \\ \hat{H}^{(I)}(z) &= \sum_{i \in I} \left[\frac{1}{2} \sum_{\text{all } j} [\mathcal{E}_{ij}^O(z) |i\rangle \langle j| + \mathcal{E}_{ji}^O |j\rangle \langle i|] + \mathcal{E}_{ii}^D(z) |i\rangle \langle i| \right] \\ &\quad + \sum_{l \notin I} \left[\frac{1}{2} \sum_{\text{all } j} (T_{lj} |l\rangle \langle j| + T_{jl} |j\rangle \langle l|) + V_l |l\rangle \langle l| \right], \\ \delta \hat{H}^{(I)}(z) &= \sum_{i \in I} \left[\frac{1}{2} \sum_{\text{all } j} \{ [T_{ij} - \mathcal{E}_{ij}^O(z)] |i\rangle \langle j| + [T_{ji} - \mathcal{E}_{ji}^O(z)] |j\rangle \langle i| \} + [V_i - \mathcal{E}_{ii}^D(z)] |i\rangle \langle i| \right]. \end{aligned} \quad (4.1)$$

The $\frac{1}{2}$ factors result from a symmetrization which assumes that the energy in each off-diagonal bond is shared equally by the connected atoms. Decomposition (4.1) induces a Lippmann-Schwinger series for $\hat{G}(z)$,

$$\hat{G}(z) = \hat{G}^{(I)}(z) + \hat{G}^{(I)}(z) \delta \hat{H}^{(I)}(z) \hat{G}(z), \quad (4.2)$$

of which are

$$\begin{aligned} \int_{-\infty}^{\infty} d\omega \operatorname{Im} \Sigma(\vec{k}, \omega) &= -\pi Q_1(\vec{k}), \\ \int_{-\infty}^{\infty} d\omega \omega \operatorname{Im} \Sigma(\vec{k}, \omega) &= -\pi Q_2(\vec{k}), \end{aligned} \quad (3.19)$$

etc. The real parts of the sum rules may be recovered from (3.19) and the Kramers-Kronig relation implied by (3.13) as follows:

$$\operatorname{Re} \Sigma(\vec{k}, \omega) = \langle \vec{k} | \hat{H} | \vec{k} \rangle + \frac{1}{\pi} \mathcal{P} \int_{-\infty}^{\infty} d\omega' \frac{\operatorname{Im} \Sigma(\vec{k}, \omega')}{\omega' - \omega}. \quad (3.20)$$

It is also useful to note that (3.20) may be used to rewrite (3.13) as

$$\Sigma(\vec{k}, z) = \langle \vec{k} | \hat{H} | \vec{k} \rangle + \frac{1}{\pi} \int_{-\infty}^{\infty} d\omega' \frac{\operatorname{Im} \Sigma(\vec{k}, \omega')}{\omega' - z}, \quad (3.21)$$

which implies that $\Sigma(\vec{k}, z)$ has the Herglotz property ($\operatorname{Im} \Sigma < 0$ for $\operatorname{Im} z > 0$) whenever $\operatorname{Im} \Sigma(\vec{k}, z)$ is negative semidefinite on the real axis $z = \omega + i0^+$.

IV. CLUSTER EMBEDDING

We embed the central cluster in the effective medium using a technique first developed by Kumar and Joshi.²⁰ This method was used previously by Bloom and Mattis,¹⁸ and has been discussed in some detail by Bloom.¹⁷ Our implementation differs in form and is simpler than that of previous authors. In Appendix A we establish equivalency.

One begins by identifying the cluster of atoms whose internal scatterings are to be subjected to exact treatment. For a Hamiltonian of form (2.1) we group the cluster-site indices i_1, i_2, i_3, \dots in a set denoted I . The following manipulations succeed in replacing the real atoms of set I by fictitious ones characterized with the effective-medium off-diagonal matrix elements \mathcal{E}_{ij}^O and diagonal ones \mathcal{E}_{ii}^D . Hamiltonian (2.1) is written

where

$$\hat{G}^{(I)}(z) = \frac{1}{z - \hat{H}^{(I)} + i0^+}. \quad (4.3)$$

The embedding procedure is completed with the replacement (an approximation) of $\hat{G}^{(I)}(z)$ in (4.2) with the medium propagator $\hat{\mathcal{G}}(z)$ which satisfies

$$\langle \vec{k} | \hat{\mathcal{G}}(z) | \vec{k}' \rangle = \mathcal{G}_{\vec{k}, \vec{k}'}(z) = \frac{\delta_{\vec{k}, \vec{k}'}}{z - \mathcal{E}(\vec{k}, z)}, \quad (4.4)$$

with

$$\mathcal{E}(\vec{k}, z) = \langle \vec{k} | \hat{\mathcal{E}}(z) | \vec{k} \rangle, \quad (4.5)$$

$$\hat{\mathcal{E}}(z) = \hat{\mathcal{E}}^0(z) + \hat{\mathcal{E}}^D(z), \quad (4.6)$$

$$\hat{\mathcal{E}}^0(z) = \sum_{i,j=1}^N \mathcal{E}_{ij}^0(z) (1 - \delta_{ij}) |i\rangle \langle j|, \quad (4.7)$$

$$\hat{\mathcal{E}}^D(z) = \sum_{i=1}^N \mathcal{E}_{ii}^D(z) |i\rangle \langle i|.$$

Note that the range of tight-binding matrix elements \mathcal{E}_{ij}^0 will generally not coincide with that of T_{ij} . This point will be discussed in Sec. V.

For a cluster of arbitrary size, the solution of (4.2) with $\hat{G}^{(N)}(z)$ replaced by $\hat{\mathcal{G}}(z)$ assumes the form

$$\begin{aligned} \hat{G} |i_n\rangle &= \hat{\mathcal{G}} |i_n\rangle + \sum_m \hat{\mathcal{G}} |i_m\rangle \langle i_m | \frac{1}{2} (\hat{T} - \hat{\mathcal{E}}^0) \hat{G} |i_n\rangle \\ &+ \sum_m \hat{\mathcal{G}} [\frac{1}{2} (\hat{T} - \hat{\mathcal{E}}^0) + \hat{V} - \hat{\mathcal{E}}^D] |i_m\rangle \langle i_m | \hat{G} |i_n\rangle, \end{aligned} \quad (4.8)$$

in which the right-hand-side matrix elements involving \hat{G} are obtained from the coupled equations

$$\begin{aligned} \sum_m \{ \delta_{im} - \langle i_l | \hat{\mathcal{G}} [\frac{1}{2} (\hat{T} - \hat{\mathcal{E}}^0) + \hat{V} - \hat{\mathcal{E}}^D] |i_m\rangle \} \langle i_m | \hat{G} |i_n\rangle - \sum_m \langle i_l | \hat{\mathcal{G}} |i_m\rangle \langle i_m | \frac{1}{2} (\hat{T} - \hat{\mathcal{E}}^0) \hat{G} |i_n\rangle &= \langle i_l | \hat{\mathcal{G}} |i_n\rangle, \\ - \sum_m \langle i_l | \frac{1}{2} (\hat{T} - \hat{\mathcal{E}}^0) \hat{\mathcal{G}} [\frac{1}{2} (\hat{T} - \hat{\mathcal{E}}^0) + \hat{V} - \hat{\mathcal{E}}^D] |i_m\rangle \langle i_m | \hat{G} |i_n\rangle & \\ + \sum_m [\delta_{im} - \langle i_l | \frac{1}{2} (\hat{T} - \hat{\mathcal{E}}^0) \hat{\mathcal{G}} |i_m\rangle] \langle i_m | \frac{1}{2} (\hat{T} - \hat{\mathcal{E}}^0) \hat{G} |i_n\rangle &= \langle i_l | \frac{1}{2} (\hat{T} - \hat{\mathcal{E}}^0) \hat{\mathcal{G}} |i_n\rangle. \end{aligned} \quad (4.9)$$

Indices i_l, i_m , and i_n range over the cluster indexing set I . In the 1SCA, Eqs. (4.9) define a 2×2 matrix equation whose solution is

$$\begin{aligned} G_{ij}(\omega) &= \langle i | \hat{G}(\omega) | j \rangle = \{ 1 - \langle i | \frac{1}{2} [\hat{T} - \hat{\mathcal{E}}^0(\omega)] \hat{\mathcal{G}}(\omega) | i \rangle \} \mathcal{G}_{ij}(\omega) + \langle i | \frac{1}{2} [\hat{T} - \hat{\mathcal{E}}^0(\omega)] \hat{\mathcal{G}}(\omega) | j \rangle \mathcal{G}_{ii}(\omega) / R(\omega), \\ R(\omega) &= (1 - \langle i | \hat{\mathcal{G}}(\omega) \{ \frac{1}{2} [\hat{T} - \hat{\mathcal{E}}^0(\omega)] + \hat{V} - \hat{\mathcal{E}}^D(\omega) \} | i \rangle) \{ 1 - \langle i | \frac{1}{2} [\hat{T} - \hat{\mathcal{E}}^0(\omega)] \hat{\mathcal{G}}(\omega) | i \rangle \} \\ &- \langle i | \frac{1}{2} [\hat{T} - \hat{\mathcal{E}}^0(\omega)] \hat{\mathcal{G}}(\omega) \{ \frac{1}{2} [\hat{T} - \hat{\mathcal{E}}^0(\omega)] + \hat{V} - \hat{\mathcal{E}}^D(\omega) \} | i \rangle \mathcal{G}_{ii}(\omega). \end{aligned} \quad (4.10)$$

i labels the single cluster site.

V. CHOICE OF EFFECTIVE MEDIUM

Although the concepts discussed in this section are general, most of the equations shown pertain to the one-dimensional lattice. The principal point of departure of this work from that of our predecessors¹³⁻¹⁸ lies in our use of the exact sum rules for the quasiparticle self-energy, Eqs. (3.19), to determine the effective-medium self-energy function $\mathcal{E}(\vec{k}, \omega)$. Of course, use of a few sum rules is not able to completely fix the frequency dependence of \mathcal{E} . However, following Bloom and Mattis^{17,18} we find that physically intuitive arguments may be used to guess at simple parametrized forms for $\text{Im}\mathcal{E}(\omega)$ (also see Appendix B). The few $\text{Im}\mathcal{E}$ parameters may then be fixed over the entire range of model parameters (Sec. II) using the same few number of moment equations. The requirement that the effective medium be causal fixes $\text{Re}\mathcal{E}(\omega)$ via the Kramers-Kronig relation (3.20), applied to $\mathcal{E}(\vec{k}, \omega)$. Finally, physical results are obtained by explicitly averaging system functions such as $G_{ij}(\omega)$ over all appropriately weighted cluster configurations. As will be seen in the following section, the numerical results obtained from this first step in the $\text{Im}\mathcal{E}$ iterative scheme can be surprisingly good both in the weak- and strong-scattering limits. For the self-consistent implementation of this theory to be explored in subsequent work,²² we

denote by $\mathcal{E}_1(\vec{k}, \omega)$ the sum-rule-determined medium self-energy, and by $\hat{G}(\omega; n)$ the cluster propagator obtained from (4.8) with $\hat{\mathcal{G}}$ replaced by $\hat{\mathcal{G}}(\omega, n)$, Eq. (4.4), and $\hat{\mathcal{E}}_n$ replacing $\hat{\mathcal{E}}$ in both equations. Here, $n=1, 2, 3, \dots$ is the iteration index. Iterations are obtained from (3.11) in the form

$$\text{Im}\mathcal{E}_{n+1}(\vec{k}, \omega) = -\text{Im} \left[\frac{1}{[\langle \vec{k} | \hat{G}(\omega; n) | \vec{k} \rangle]_{\text{av}}} \right]. \quad (5.1)$$

The Kramers-Kronig relation (3.20) is used to compute $\text{Re}\mathcal{E}_{n+1}(\vec{k}, \omega)$, while the equations of Sec. IV determine $\hat{G}(\omega; n+1)$. Observe that in this straightforward implementation of self-consistency, the sum rules are used only initially for the determination of \mathcal{E}_1 .

Conceptually, one of the more satisfying results of the sum-rule analysis is that unlike the frequency dependence of $\mathcal{E}(\vec{k}, \omega)$, its dependence on \vec{k} is completely fixed in "each order" of approximation. Here, "each order" does not refer to cluster size but rather to the number of sum rules invoked. If the disordered matrix elements of T_{ij} occur only between nearest neighbors, we find that the weak-scattering limit (overlapping impurity bands) is described sufficiently well with the use of only the first sum rule, which produces an effective medium with off-diagonal matrix elements between first and second nearest neighbors. In the strong-scattering limit (nonoverlapping

impurity bands) and the same T_{ij} , two sum rules are minimally required, producing an effective medium with matrix elements between first-, second-, and third-nearest neighbors. For the one-dimensional case, the sum-rule analysis proceeds as follows.

We rewrite Eqs. (3.8)–(3.10) in the form

$$\langle k_x | (\hat{H})^m | k_x \rangle = \sum_{n=0}^m A_{mn} \cos(nak_x), \quad m = 1, 2, \dots \quad (5.2)$$

The coefficients A_{mn} are, from (3.8)–(3.10),

$$A_{10} = \sum_{\alpha=A,B} c_\alpha V_\alpha, \quad A_{11} = 2 \sum_{\alpha} c_\alpha \sum_{\beta=A,B} P(\beta; \alpha) T_{\alpha\beta}, \quad (5.3)$$

$$A_{20} = \sum_{\alpha} c_\alpha \left[V_\alpha^2 + 2 \sum_{\beta} P(\beta; \alpha) T_{\alpha\beta} T_{\beta\alpha} \right],$$

etc. We rewrite Eqs. (3.16) in the form

$$Q_m(k_x) = \sum_{n=0}^{m+1} S_{mn} \cos(nak_x), \quad m = 0, 1, \dots \quad (5.4)$$

with the coefficients given by

$$\begin{aligned} S_{00} &= A_{10}, \quad S_{01} = A_{11}, \\ S_{10} &= A_{20} - A_{10}^2 - \frac{1}{2} A_{11}^2, \quad S_{11} = A_{21} - 2A_{10}A_{11}, \\ S_{12} &= A_{22} - \frac{1}{2} A_{11}^2, \quad S_{1n} = 0 \quad \text{for } n \geq 3, \\ S_{20} &= A_{30} - A_{10}^3 - 2A_{10}S_{10} - \frac{3}{2} A_{10}A_{11}^2 - A_{11}S_{11}, \quad (5.5) \\ S_{21} &= A_{31} - 3A_{10}^2A_{11} - 2(A_{10}S_{11} + A_{11}S_{10}) \\ &\quad - \frac{3}{4} A_{11}^3 - A_{11}S_{12}, \\ S_{22} &= A_{32} - 2A_{10}S_{12} - \frac{3}{2} A_{10}A_{11}^2 - A_{11}S_{11}, \\ S_{23} &= A_{33} - \frac{1}{4} A_{11}^3 - A_{11}S_{12}, \quad S_{2n} = 0 \quad \text{for } n \geq 4, \end{aligned}$$

etc. The moment equations (3.19) for the effective medium assume the form

$$\int_{-\infty}^{\infty} d\omega \omega^{m-1} \text{Im} \mathcal{E}(k_x, \omega) = -\pi \sum_{n=0}^{m+1} S_{mn} \cos(nak_x), \quad m = 1, 2, \dots \quad (5.6)$$

Our ansatz for $\text{Im} \mathcal{E}(k_x, \omega)$ is, in the one-dimensional case,

$$\text{Im} \mathcal{E}(k_x, \omega) = \sum_{n=0}^{M+1} f_n(\omega) \cos(nak_x), \quad (5.7)$$

where the $f_n(\omega)$ are simple functional forms which we discuss below. In Eq. (5.7), M is the number of moment

$$f_n^2(\omega) = \begin{cases} \beta_n, & \Omega_1 < \omega < \Omega_2 \\ \frac{1}{\Omega_3 - \Omega_2} [\beta_n(\Omega_3 - \omega) + \alpha_n(\omega - \Omega_2)], & \Omega_2 < \omega < \Omega_3 \\ \alpha_n, & \Omega_3 < \omega < \Omega_4 \\ 0, & \text{otherwise.} \end{cases} \quad (5.12)$$

The first two moment equations (5.6) require that the constants β_n, α_n satisfy

equations used to construct a given approximation. Expression (5.7) is consistent with the structure of the $Q_m(k_x)$, Eq. (5.4), and the independence of the substitutional from the topological properties of our model. In the determination of $f_n(\omega)$ there arises the question of band edges. It is evident that the iterative, self-consistent implementation of this theory contains a description of band-edge effects. However, for our present purpose we limit the bands by the theoretical band limits obtained from Gershgorin's theorem.^{1,23} Once the parameters occurring in $f_n(\omega)$ have been fixed, using sum rules (5.6), the Kramers-Kronig relation (3.20) is used to determine

$$\begin{aligned} \text{Re} \mathcal{E}(k_x, \omega) &= \langle k_x | \hat{H} | k_x \rangle \\ &+ \sum_{n=0}^{M+1} \left[\frac{1}{\pi} \text{P} \int_{-\infty}^{\infty} d\omega' \frac{f_n(\omega')}{\omega' - \omega} \right] \cos(nak_x). \end{aligned} \quad (5.8)$$

In Sec. VI we present numerical results obtained for two distinct effective mediums. Visibly, our choices have been influenced by the work of Bloom and Mattis,^{17,18} however, other choices are also possible. Consideration of a few of these, including a discussion of simple criteria which are helpful in guiding a selection of $\mathcal{E}(\vec{k}, \omega)$, is found in Appendix B.

(a) *Medium 1.* This medium is suitable for description of the weak-scattering, single-impurity-band limit. This medium is fixed using only the first moment equation (5.6) so that $M = 1$ in Eq. (5.7). Denoting Ω_1 and Ω_2 to be the theoretical band edges, we take

$$\text{Im} \mathcal{E}^1(k_x, \omega) = \sum_{n=0}^2 f_n^1(\omega) \cos(nak_x), \quad (5.9)$$

with

$$f_n^1(\omega) = \begin{cases} -\pi \frac{S_{1n}}{\Omega_2 - \Omega_1}, & \Omega_1 < \omega < \Omega_2, \quad n = 0, 1, 2 \\ 0, & \text{otherwise.} \end{cases} \quad (5.10)$$

(b) *Medium 2.* This medium is suitable for description of the strong-scattering, split-band limit. Two moment equations are required so that $M = 2$. Let Ω_1, Ω_2 denote the edges of the lower-frequency band and Ω_3, Ω_4 denote the edges of the upper-frequency band; then

$$\text{Im} \mathcal{E}^2(k_x, \omega) = \sum_{n=0}^3 f_n^2(\omega) \cos(nak_x), \quad (5.11)$$

with

$$\begin{aligned}
[\Omega_2 - \Omega_1 + \frac{1}{2}(\Omega_3 - \Omega_2)]\beta_n + [\Omega_4 - \Omega_3 + \frac{1}{2}(\Omega_3 - \Omega_2)]\alpha_n &= -\pi S_{1n}, \quad n=0,1,2,3 \\
[\Omega_2^2 - \Omega_1^2 + \frac{1}{3}(\Omega_3 - \Omega_2)(\Omega_3 + 2\Omega_2)]\beta_n + [\Omega_4^2 - \Omega_3^2 + \frac{1}{3}(\Omega_3 - \Omega_2)(2\Omega_3 + \Omega_2)]\alpha_n &= -2\pi S_{2n}.
\end{aligned}
\tag{5.13}$$

In Fig. 1 we display $f_n^2(\omega)$.

In view of our numerical results, it is interesting to observe that the postulate of a nonvanishing $\text{Im}\mathcal{E}$ in the gap region (Ω_2, Ω_3) between the separated subbands seems necessary in order to satisfy the local density-of-states sum rule, Eq. (6.2). In the split-band limit, all of our attempts at guessing simply parametrized functional forms of $\text{Im}\mathcal{E}$ within the bands with $\text{Im}\mathcal{E}=0$ in the gap have failed to satisfy (6.2). This result is suggestive of the existence of some singular structure in the self-consistent $\mathcal{E}(\vec{k}, z)$ for z exactly on the real axis within the gap region. It is known that the CPA yields an isolated singularity there, in the limit of uncorrelated diagonal disorder.¹⁹ In the CPA case, it is found that for each \vec{k} , the infinite set of matrix elements $\langle \vec{k} | \hat{H}^n | \vec{k} \rangle$ are required to fix both the strength and position of the singularity on the real axis. Should the existence of such singular structure prove to be a general feature of cluster mean-field theories, the arguments of Velicky *et al.*¹⁹ indicate that, for off-diagonal and/or correlated disorder, a distribution of singularities, with a separate one for each \vec{k} , might be expected. Such singular structure would explain our results. From our point of view, its primary function would be an effective renormalization of the right-hand side of the moment equations (3.19) to ensure the satisfaction of Eq. (6.2). This is precisely what is accomplished by the presence of a nonzero $\text{Im}\mathcal{E}$ in the gap. Note also that in the limit of connected subbands, when the gap is absent, seemingly any choice of $\text{Im}\mathcal{E}$ will satisfy the density-of-states sum rule, if the low-order moment equations are obeyed, and if $\text{Im}\mathcal{E}$ is nonzero within the band. These matters should become clearer on implementation of self-consistency.²²

VI. NUMERICAL RESULTS

We confine ourselves to density-of-states results obtained for the one-dimensional disordered alloy of Sec. II in the 1SCA. First, we show that use of the sum rules, as outlined in the preceding section, yields an effective medium which is meaningfully dependent on the model parameters of Sec. II. We restrict the following considerations to mediums 1 and 2 defined in Sec. V.

It is well known that the imaginary part of the self-energy $\Sigma_{\vec{k}}$ is inversely proportional to the lifetime of an

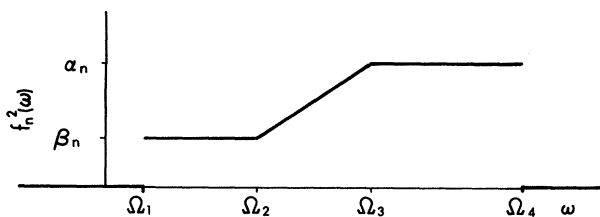


FIG. 1. The medium 2, $f_n^2(\omega)$ is displayed.

excitation in the quasiparticle state with wave vector \vec{k} . Therefore, we expect that for the model alloy of Sec. II, the disorder-induced lifetimes will diverge in the majority subband as the concentration of the minority component is allowed to vanish. Fig. 2 shows the concentration dependence of f_0^1 , Eq. (5.10), for the case of diagonal disorder only: $T_{ij}=1.0$, in the weak-scattering limit $V_A = -V_B = 0.5$, and in the absence of correlation, $s=0$. We note that $\text{Im}\mathcal{E}$ is symmetric about concentration 0.5, reflecting the symmetry of the model parameters, and that it vanishes at extreme values of the concentration of either component. The corresponding result for medium 2, Eqs. (5.11) and (5.12), is shown in Fig. 3 when $T_{ij}=1.0$, $V_A = -V_B = 2.5$, and $s=0$. The figure depicts the dependence on the A -atom concentration of $\text{Im}\mathcal{E}$ [β_0 in Eq. (5.12)] in the B subband. By symmetry, $\text{Im}\mathcal{E}$ in the A subband is obtained from a mirror reflection of the displayed curve of about $C_A=0.5$. The first two sum rules predict a causal medium 2, with the anticipated dependence on concentration, except in the extreme dilute limit of either component where causality is lost. This possible loss of causality is, of course, ansatz dependent and may be corrected with a better guess for the frequency dependence of $f_n(\omega)$ in Eq. (5.7). After all, the sum rules are all satisfied by the exact, causal $\text{Im}\Sigma(\vec{k}, \omega)$, and therefore it is no surprise that a simplified guess could cause difficulties for certain extreme values of the model parameters. We find that the presence of off-diagonal disorder and short-range order have the general effect of restricting the range of model parameters for which simple parametrizations of the frequency dependence of $f_n(\omega)$, in (5.7), result in a causal medium. This indicates to us the need to include, in our guesses of the frequency dependence of $f_n(\omega)$, certain (yet unknown) gross characteristics whose presence signals off-diagonal disorder and/or short-range order in the model. An illustrative discussion of this point will be found in Appendix B. In any case, where the sum-rule-predicted medium is causal, we have always found the expected qualitative dependence on model parameters. We should also note that these considerations

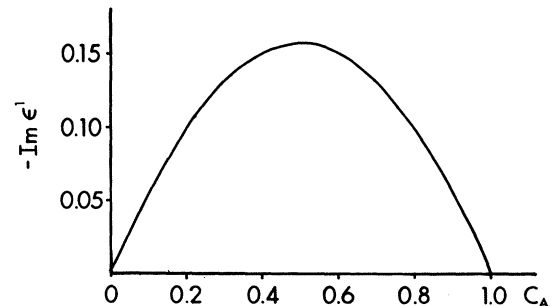


FIG. 2. We plot the sum-rule-determined $\text{Im}\mathcal{E}$ for medium 1 as a function of the concentration of A atoms. Our Hamiltonian parameters at $T_{ij}=1.0$, $V_A = -V_B = 0.5$, and $s=0$.

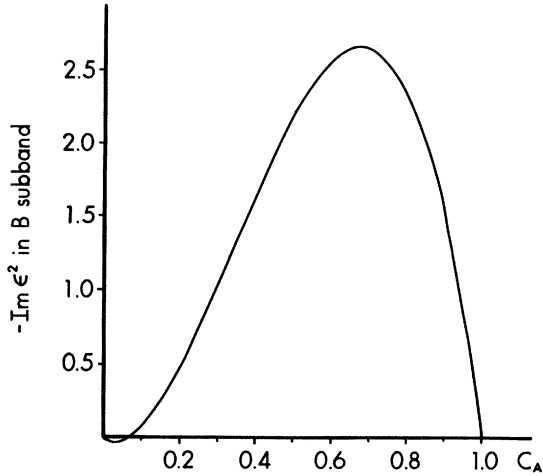


FIG. 3. Sum-rule-determined $\text{Im}\mathcal{E}^2$ in the B band shown as a function of A -atom concentration. The model parameters are $T_{ij}=1.0$, $V_A=-V_B=2.5$, and $s=0$. Causality may be violated for a sufficiently poor guess for the frequency dependence of $\text{Im}\mathcal{E}(\vec{k},\omega)$.

are considerably less significant for self-consistent, iterative applications of the method. There, the sum rules are invoked only in the first step to obtain an initial guess. If a causal medium is not obtained from the sum rules for the desired set of model parameters, a causal medium for some different set of parameters should serve as well, to initiate the process. In the limit of only diagonal disorder, the sum rules predict that $\text{Im}\mathcal{E}(\omega)$ is independent of k_x . This is an exact result which does not depend on our ansatz for the frequency dependence of $\text{Im}\mathcal{E}$, nor does it depend on scattering strength.

It is interesting to observe that for the Hamiltonian parameters of Fig. 2, Bloom and Mattis^{17,18} obtained their best results for $c_A=c_B=0.5$ with a guessed value

$|\text{Im}\mathcal{E}|=0.15$. This is to be compared with our sum-rule-determined value of 0.157. The 1SCA local density of states, which we compute for the parameters of Fig. 2 and $c_A=0.5$, is essentially identical to the top of Fig. 2 of Ref. 18. In Figs. 4 and 5, we show our medium-2 (Fig. 1) strong-scattering results for the 1SCA local density of states,

$$\rho(\omega) = -\frac{1}{\pi} \text{Im}[\langle i | \hat{G}(\omega) | i \rangle]_{\text{av}} \quad (6.1)$$

in the presence of diagonal and off-diagonal disorder, respectively. Our results are compared with essentially exact histograms taken from the work of Kaplan, Leath, Gray, and Diehl.¹¹ The dashed line is the sum-rule-determined input density of states of the medium, while the solid curve is the first-iteration result. We observe the atomiclike peak in the minority band and also a very good description of the mean shape of the spectrum. The finite density of states in the interband gap (solid curve) is due to our having ascribed a nonzero density of states to the medium there (dashed curve). The first-iteration density of states in the gap is significantly smaller than that of the guessed medium indicating an approach towards 0 with further iterations. Within numerical accuracy, the density-of-states sum rule

$$\int_{-\infty}^{\infty} d\omega \rho(\omega) = 1 \quad (6.2)$$

is satisfied by the solid curves of both Figs. 4 and 5.

VII. SUMMARY

We have developed a simple, computational, and iteratively self-consistent method to calculate the physical properties of disordered systems in which the distribution of disorder is translationally invariant. The theory encompasses diagonal and off-diagonal disorder with arbitrary specification of short-range-order distribution functions. Substitutional as well as amorphous systems may be studied with this method. We have shown strong-

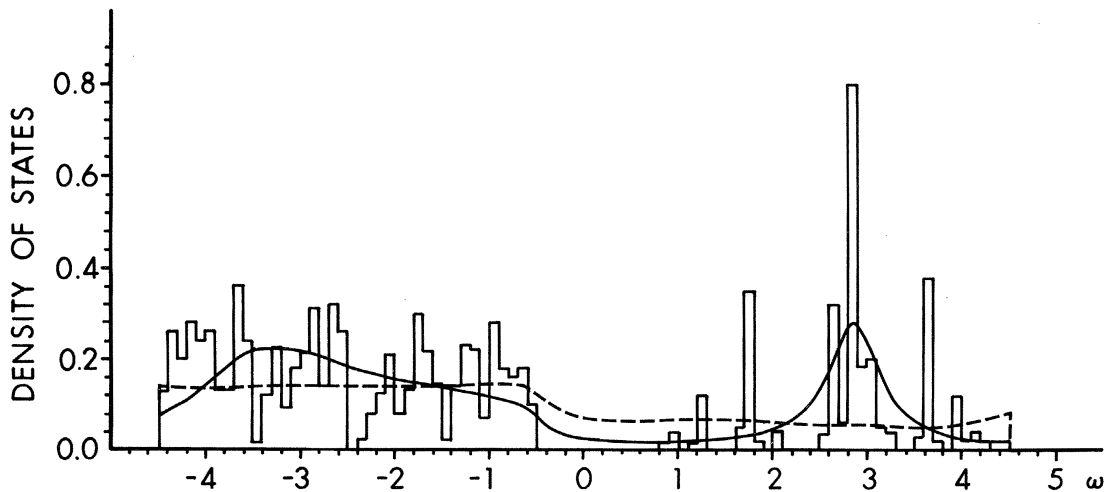


FIG. 4. First-iteration result (solid curve) for the single-particle-cluster approximation is shown for $T_{ij}=1.0$, $V_A=-V_B=2.5$, $C_A=0.3$, and $s=0$. The dashed curve is the sum-rule-determined, effective-medium density of states which was used as input to obtain the solid curve. The essentially exact histogram is taken from Ref. 11.

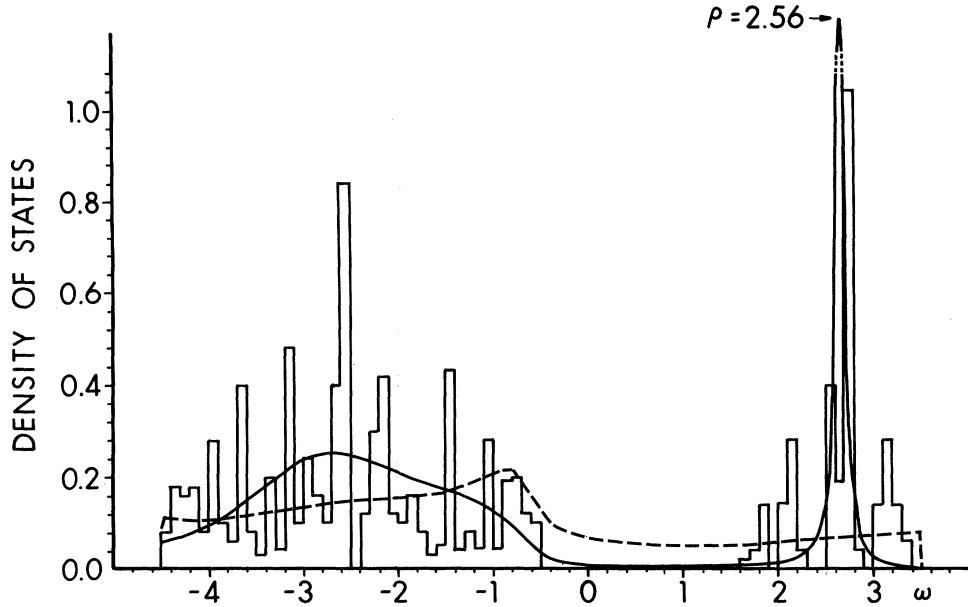


FIG. 5. Same as Fig. 4, except for the presence of off-diagonal disorder: $T_{AA}=T_{AB}=T_{BA}=0.5$ and $T_{BB}=1.0$.

scattering numerical results for the density of states in the single-site-cluster approximation for diagonal and off-diagonal disorder. A planned, forthcoming paper will present the corresponding numerical results for short-range order in multiple-site-cluster approximations. This work has established the usefulness and computational practicability of the sum-rule method for the study of the energy spectrum of disordered systems. As a one-step procedure, the scheme is approximate and analytic by construction. As found here and also by other authors,^{17,18} first-iteration results can be remarkably good. For each chosen cluster size, self-consistent results are possible through repeated iteration. In future work we shall explore this iterative self-consistency, as well as transport in substitutional and amorphous systems, and the application of this technique to geophysical problems of current interest.

ACKNOWLEDGMENTS

I am very grateful to Dr. Raghu Raghavan for the many discussions that we have had on various technical aspects of this theory. His help in guiding me through the literature has been invaluable. I also thank Dr. Robert Euwema for his incisive comments and his patience with my frequent impositions on his time, and Dr. Theodore Kaplan for helpful discussions. This study was supported in part by Grant No. DAAHO1-80-C-0493 of the U. S. Department of Defense Advance Research Projects Agency while the author was a consultant to Riverside Research Institute, New York.

APPENDIX A

Here we establish the equivalence of our embedding technique, discussed in Sec. IV, with that of previous authors.^{17,18,20} Consider, for illustration, the treatment of a

cluster of two atoms labeled 1 and 2. The standard technique develops the Green's function $\hat{G}(z)$ in a hierarchical series

$$\hat{G} = \hat{G}^{(1)} + \hat{G}^{(1)} \delta \hat{H}^{(1)} \hat{G}, \quad (\text{A1})$$

$$\hat{G}^{(1)} = \hat{G}^{(1,2)} + \hat{G}^{(1,2)} \delta \hat{H}^{(2)} \hat{G}^{(1)},$$

where in the notation of Sec. IV, $\hat{G}^{(1)}$ is $\hat{G}^{(I)}$ when $(I) = \{1\}$, $\hat{G}^{(1,2)}$ is $\hat{G}^{(I)}$, when $(I) = \{1,2\}$, etc. A simple manipulation recasts (A1) to a form

$$\hat{G} = \hat{G}^{(1,2)} + \hat{G}^{(1,2)} (\delta \hat{H}^{(1)} + \delta \hat{H}^{(2)}) \hat{G}, \quad (\text{A2})$$

which is identical to (4.2) since by definitions (4.1), $\delta \hat{H}^{(I)}$ is additive over $i \in I$, and $\hat{H}^{(I)}$ does not depend on the order with which atoms are inducted into the cluster. The reader will easily verify that form (A2) is independent of the number of equations included in the hierarchy (A1).

APPENDIX B

The infinite set of moment-equations (3.19) completely determine the wave-vector and frequency dependence of the imaginary part of the exact self-energy $\Sigma(\vec{k}, \omega)$. Its real part is fixed by the Kramers-Kronig relation (3.20). Formally this follows from (3.21); however, rigorous statements may be found in Ref. 24. A natural question is how much of the structure of $\Sigma(\vec{k}, \omega)$ is determined by the first few moment equations? Or more precisely, to what extent do the first few moment equations limit the frequency dependence of $\text{Im}\Sigma(\vec{k}, \omega)$? We limit this discussion to the one-dimensional case when two moment equations are invoked. It turns out that our ansatz (5.7) for $\text{Im}\mathcal{E}$.

$$\text{Im}\mathcal{E}(k_x, \omega) = \sum_{n=0}^{\infty} f_n(\omega) \cos(nak_x), \quad (\text{B1})$$

is, in fact, exact due to the requirements that \mathcal{E} is invariant under translation by a reciprocal-lattice vector and under reflection about $k_x=0$. From (5.6) and (5.7), two moment equations yield four independent sets of two equations each,

$$\int_{-\infty}^{\infty} d\omega f_n(\omega) = -\pi S_{1n},$$

$$\int_{-\infty}^{\infty} d\omega \omega f_n(\omega) = -\pi S_{2n}, \quad n=0,1,2,3. \quad (\text{B2})$$

As the S_{mn} are all positive semidefinite (numerically this is invariably the case, although we have no formal proof), it is not a difficult matter to guess at simple parametrized forms $f_n(\omega)$ satisfying (B2). Once parameters have been determined by (B2), the trial functional form of $\text{Im}\mathcal{E}(k_x, \omega)$ is given by (5.7), with $M=2$. At this point, a new constraint must be imposed on the set of $f_n(\omega)$, namely that at each ω the sum in (5.7) yields a negative semidefinite value for all values of $0 \leq ak_x \leq 2\pi$. We find that this causal-mode condition is a strong constraint for systems with off-diagonal disorder and/or short-range order. The implication being that some very specific information as to the character of the disorder under study is coded into gross features of the overall shape of $\text{Im}\Sigma(k_x, \omega)$. Should this effect survive the transition from one-dimensional to three-dimensional systems, it is conceivably of some experimental importance. For theoretical purposes, the strength of this causal-mode condition is most felt when undertaking studies of trend behavior in which Hamiltonian and/or disorder parameters are allowed to vary over their entire breadth in range. For then, this moment technique requires functions $f_n(\omega)$ which yield mode causality over the entire parameter space. With the use of three moment equations on a system with off-diagonal disorder, it is not too difficult to find simple functions $f_n(\omega)$ which give mode causality over restricted ranges of constituent concentration. However, we have not yet succeeded in guessing a suitable set of functions with mode causality over all concentration ranges. This explains the conspicuous absence of numerical results for three moment equations in this work.

We illustrate the above discussion with an example. Consider an off-diagonally disordered system with $T_{AA}=1.0$, $T_{AB}=T_{BA}=0.6$, $T_{BB}=0.2$, $V_A=-V_B=1.0$, and without correlation $s=0$. Gershgorin's theorem²³ gives two partially overlapping bands $(\Omega_1, \Omega_2)=(-2.2, 0.2)$ and $(\Omega_3, \Omega_4)=(-1.0, 3.0)$. As a first guess we take a simple functional form

$$f_n^I(\omega) = B_n^I(\omega) + A_n^I(\omega),$$

$$B_n^I(\omega) = \begin{cases} \beta_n, & \Omega_1 < \omega < \Omega_2 \\ 0, & \text{otherwise,} \end{cases}$$

$$A_n^I(\omega) = \begin{cases} \alpha_n, & \Omega_3 < \omega < \Omega_4 \\ 0, & \text{otherwise,} \end{cases} \quad (\text{B3})$$

where the self-energy has been taken to be a constant in each subband and additive in the overlap region. The point illustrated here is quite general and is independent of this additivity assumption. Using (B3) in (B2) one

solves for the parameters β_n, α_n . We ask over what range of concentration c_A does the resulting $\text{Im}\mathcal{E}(k_x, \omega)$, Eq. (5.7), satisfy mode causality? We find that it is satisfied for c_A in the range 0.229–1.0. At $C_A=0.228$ and for frequencies $\Omega_1 < \omega < \Omega_3$, we obtain

$$\text{Im}\mathcal{E}(k_x, \omega) = -0.0626 - 0.0796 \cos(ak_x) \\ - 0.0168 \cos(2ak_x) \\ - 3.8 \times 10^{-10} \cos(3ak_x), \quad (\text{B4})$$

which is positive (acausal) at $k_x=\pi/a$. Loss of mode causality tends to first appear at Brillouin-zone edges, although not invariably. Continuing the search for better f_n 's, we consider ones with more structure, such as

$$f_n^{\text{II}}(\omega) = B_n^{\text{II}}(\omega) + A_n^{\text{II}}(\omega),$$

$$B_n^{\text{II}}(\omega) = \begin{cases} \beta_n [(\omega - \Omega_1)/(\Omega_b - \Omega_1)], & \Omega_1 < \omega < \Omega_b \\ \beta_n [(\Omega_2 - \omega)/(\Omega_2 - \Omega_b)], & \Omega_b < \omega < \Omega_2 \\ 0, & \text{otherwise,} \end{cases}$$

$$A_n^{\text{II}}(\omega) = \begin{cases} \alpha_n [(\omega - \Omega_3)/(\Omega_a - \Omega_3)], & \Omega_3 < \omega < \Omega_a \\ \alpha_n [(\Omega_4 - \omega)/(\Omega_a - \Omega_b)], & \Omega_a < \omega < \Omega_4 \\ 0, & \text{otherwise.} \end{cases} \quad (\text{B5})$$

A triangular form is assigned to each band with additivity in the overlap. The four triangles in the B subband ($n=0,1,2,3$) have their cusps at $\omega=\Omega_b$, while those in the A subband have their cusps at $\omega=\Omega_a$. Parameters Ω_b and Ω_a shall be considered adjustable. They parametrize the overall shape of the f_n 's. For each selected pair of Ω_b and Ω_a , the moment equations (B2) are applied, as before, to the determination of the triangle heights β_n and α_n . As a first guess using form (B5), we take Ω_b and Ω_a in the center of their respective bands and search for the range of c_A satisfying mode causality. We find that the causal range of c_A is unchanged (0.229–1.0). We now shift Ω_b to various different values in its allowed range ($-2.2, 0.2$), and for each choice test for the causal range concentration c_A . Again, it is unchanged indicating that failure of mode causality at small concentrations c_A is probably not due to our poor guess of the overall shape of Σ over the range of frequencies corresponding to subband B . When c_A is small, causality does not impose a significant condition on the overall frequency dependence of Σ in the range ($-2.2, 0.2$). Applying this analysis to the A subband produces a striking result. We choose $\Omega_b=1.0$, at the center of subband B , and vary Ω_a . We find that the causal range of c_A is extremely sensitive to the overall frequency dependence of Σ in subband A . When $\Omega_a=-0.9$, the range of causal c_A is diminished to (0.727–1.0), while if $\Omega_a \geq 1.94$, all concentrations of c_A are causal. If Ω_a is decreased slightly below 1.94, causality fails first at $ak_x \simeq 2.2$. These results suggest that at small values of c_A the exact $\Sigma(k_x, \omega)$ should exhibit an enhanced magnitude in the frequency range (0.2, 3.0). More generally, it appears that at least for certain values of the system parameters, the requirement that all effective-medium modes be causal imposes the presence of identifiable gross characteristics in the fre-

quency dependence of $\Sigma(\vec{k}, \omega)$. This matter is expected to become clearer in self-consistent calculations.²² It should be noted that the triangular self-energy (B5) does not yield a satisfactory local density-of-states spectrum, apparently due to the rapid decrease of $\text{Im}\mathcal{E}$ near the band edges. The resulting density of states exhibits an accentuated narrowness. Therefore, it appears that the constant component of $\text{Im}\mathcal{E}$ is necessary in order to obtain good spec-

tra. Pointed structures such as (B5) should be included only as corrections to the constant component. The above analysis, which uses (B5) alone, addresses essential points while avoiding unnecessary complications. Evidently, our conclusions of this Appendix will only be quantitatively affected by the presence of the proper constant component of $\text{Im}\mathcal{E}$.

¹R. J. Elliott, J. A. Krumhansl, and P. L. Leath, *Rev. Mod. Phys.* **46**, 465 (1974).

²P. Soven, *Phys. Rev.* **156**, 809 (1967).

³D. W. Taylor, *Phys. Rev.* **156**, 1017 (1967).

⁴P. W. Anderson and W. L. McMillan, in *Theory of Magnetism in Transition Metals, Proceedings of the International School of Physics "Enrico Fermi," Course 37*, edited by H. Suhl (Academic, New York, 1967).

⁵B. G. Nickel and W. H. Butler, *Phys. Rev. Lett.* **30**, 373 (1973).

⁶R. Mills and P. Ratanavararaks, *Phys. Rev. B* **18**, 5291 (1978).

⁷A. Mookerjee, *J. Phys. C* **6**, L205 (1973).

⁸A. Mookerjee, *J. Phys. C* **6**, 1340 (1973).

⁹T. Kaplan and L. J. Gray, *Phys. Rev. B* **14**, 3462 (1976); **15**, 6005 (1977).

¹⁰H. W. Diehl and P. L. Leath, *Phys. Rev. B* **19**, 587 (1979); **19**, 596 (1979).

¹¹T. Kaplan, P. L. Leath, L. J. Gray, and H. W. Diehl, *Phys. Rev. B* **21**, 4230 (1980).

¹²L. J. Gray and T. Kaplan, *Phys. Rev. B* **24**, 1872 (1981).

¹³J. D. Joannopoulos and F. Yndurain, *Phys. Rev. B* **10**, 5164

(1974).

¹⁴L. M. Falicov and F. Yndurain, *Phys. Rev. B* **12**, 5664 (1975).

¹⁵P. N. Sen and F. Yndurain, *Phys. Rev. B* **13**, 4387 (1976).

¹⁶A. Gonis and J. W. Garland, *Phys. Rev. B* **16**, 2424 (1977).

¹⁷P. Bloom, Ph.D. thesis, Yeshiva University, 1977.

¹⁸P. Bloom and D. C. Mattis, *Phys. Rev. B* **15**, 3633 (1977).

¹⁹B. Velicky, S. Kirkpatrick, and H. Ehrenreich, *Phys. Rev.* **175**, 747 (1968).

²⁰V. Kumar and S. K. Joshi, *J. Phys. C* **8**, L148 (1975).

²¹There are a few misprints in Appendix 2 of Ref. 8. On the second line, β_0 should replace ρ_0 at the top of p. 1349, one should read

$$g(z) = z/\beta_0 + \int_{-\infty}^{\infty} [(1+\tau z)/(\tau-z)] d\gamma(\tau) + C \\ = Z/\beta_0 + g_1(z).$$

²²R. E. Peña (in preparation).

²³J. N. Franklyn, *Matrix Theory* (Prentice-Hall, Englewood Cliffs, N.J., 1968), p.161.

²⁴J. A. Shohat and J. D. Tamarkin, *The Problem of Moments* (American Mathematical Society, New York, 1943).